Article

Quantum phase transition and destruction of Kondo effect in pressurized SmB_6

Yazhou Zhou [a], Qi Wu [a], Priscila F.S. Rosa [b,c], Rong Yu [d,i,j], Jing Guo [a], Wei Yi [a], Shan Zhang [a], Zhe Wang [a], Honghong Wang [a], Shu Cai [a], Ke Yang [e], Aiguo Li [e], Zheng Jiang [e], Shuo Zhang [e], Xiangjun Wei [e], Yuying Huang [e], Peijie Sun [a], Yi-feng Yang [a,g], Zachary Fisk [b], Qimiao Si [a,f], Zhongxian Zhao [a,g,h], Liling Sun [a,g,h,*]

[a] Institute of Physics and Beijing National Laboratory for Condensed Matter Physics, Chinese Academy of Sciences, Beijing 100190, China
[b] Department of Physics and Astronomy, University of California, Irvine, CA 92697, USA
[c] Los Alamos National Laboratory, Los Alamos, NM 87545, USA
[d] Department of Physics, Renmin University of China, Beijing 100872, China
[e] Shanghai Synchrotron Radiation Facilities, Shanghai Institute of Applied Physics, Chinese Academy of Sciences, Shanghai 201204, China
[f] Department of Physics & Astronomy, Rice University, Houston, TX 77005, USA
[g] Collaborative Innovation Center of Quantum Matter, Beijing 100190, China
[h] University of Chinese Academy of Sciences, Beijing 100190, China
[i] Department of Physics and Astronomy, Shanghai Jiao Tong University, Shanghai 200240, China
[j] Collaborative Innovation Center of Advanced Microstructures, Nanjing 210093, China

ARTICLE INFO

ABSTRACT

SmB_6 has been a well-known Kondo insulator for decades, but recently attracts extensive new attention as a candidate topological system. Studying SmB_6 under pressure provides an opportunity to acquire the much-needed understanding about the effect of electron correlations on both the metallic surface state and bulk insulating state. Here we do so by studying the evolution of two transport gaps (low temperature gap E_l and high temperature gap E_h) associated with the Kondo effect by measuring the electrical resistivity under high pressure and low temperature (0.3 K) conditions. We associate the gaps with the bulk Kondo hybridization, and from their evolution with pressure we demonstrate an insulator-to-metal transition at $\sim$4 GPa. At the transition pressure, a large change in the Hall number and a divergence tendency of the electron-electron scattering coefficient provide evidence for a destruction of the Kondo entanglement in the ground state. Our results raise the new prospect for studying topological electronic states in quantum critical materials settings.

© 2017 Science China Press. Published by Elsevier B.V. and Science China Press. All rights reserved.

1. Introduction

Samarium hexaboride (SmB_6) is a paradigm Kondo insulator (KI) with a simple cubic structure, comprising a B_6 octahedral framework and Sm ions [1]. It has in common with other KIs that an insulating gap opens upon cooling due to the hybridization between the localized f-electrons and conduction electrons [2–4], but distinguishes from the other KIs by the presence of a low temperature resistance plateau which has been a puzzle for decades [5,6]. Recent theoretical studies suggest that the resistance plateau may be associated with the existence of an exotic metallic surface state, and that SmB_6 could be a new class of topological insulator with strong electron correlations, namely a topological Kondo insulator (TKI) [7,8]. A metallic surface state indeed has been con-

firmed by a variety of measurements [9–17], but whether it is protected by a non-trivial topology remains to be established [18]. Surprisingly, various energy gaps ranging from 5 to 15 meV have been observed from ambient-pressure resistivity, angle resolved photoemission spectroscopy (ARPES), and scanning tunneling spectroscopy (STS) experiments [6,19–23], but it is still unclear how these gaps relate with the bulk Kondo hybridization between $4f$ electrons and conduction electrons. In addition, the newly discovered quantum oscillation phenomena, which suggest an unusual Fermi surface in SmB_6 at low temperature, yield an additional puzzle [24,25]. In order to make progress on these issues, it is crucially important to understand the nature of the multiple electronic gaps.

One of the important means to understand Kondo hybridization gap is the tuning of the Kondo insulators through a quantum phase transition [4], in particular through the phase diagram proposed for such systems at zero temperature [26,27]. For studying

* Corresponding author.
 E-mail address: llsun@iphy.ac.cn (L. Sun).

quantum phase transition, it is known that high pressure is a "clean" way of continuously tuning the crystal and electronic structures without introducing additional chemical complexity [28,29]. Before the proposal of topological conducting surface state [5,6,21,30–33], high-pressure phenomena of SmB_6 had been extensively investigated down to 1.5 K, however a systematic understanding on the instability of the metallic surface state and Kondo hybridization bulk state is lacking. In this study we use our advanced high-pressure facilities which allow us to perform resistance measurements down to 0.3 K, and apply the *complementary* measurements – adopting the same high pressure cell, the same pressure transmitting medium and the same pressure gauge on the same batch of single crystal – to carry out such investigations on SmB_6.

2. Methods

High quality single crystals of SmB_6 were grown by the Al flux method, as described in Ref. [11]. Pressure was generated by a diamond anvil cell with two opposing anvils sitting on the Be-Cu supporting plates. Diamond anvils with 300 μm flat and non-magnetic rhenium gaskets with 100 μm diameter hole were employed for different runs of the high-pressure studies. The standard four-probe method was applied on the (0 0 1) facet of single crystal SmB_6 for all high pressure transport measurements. To keep the sample in a quasi-hydrostatic pressure environment, NaCl powder was employed as a pressure transmitting medium for the high-pressure resistance and Hall coefficient measurements.

High pressure X-ray diffraction (XRD) and X-ray absorption spectroscopy (XAS) experiments were performed at room temperature at beamline 4W2 in the Beijing Synchrotron Radiation Facility and at the beamline 14W1 in the Shanghai Synchrotron Radiation Facility, respectively. Diamonds with low birefringence were selected for the experiments. A monochromatic X-ray beam with a wavelength of 0.6199 Å was adopted for all XRD measurements. To maintain the sample in a hydrostatic pressure environment, silicon oil was used as pressure transmitting medium in the high-pressure XRD and XAS measurements. Pressure was determined by the ruby fluorescence method [34].

3. Experimental results

We first performed *in situ* high pressure resistance measurements down to low temperatures (0.3 K) on single crystal SmB_6. As demonstrated in Fig. 1a and b, the resistivity for sample A and B shows the same behavior at pressures below 4 GPa, *i.e.* the resistivity increases continuously upon decreasing temperature and then displays a plateau below ~4 K, which is consistent with the results reported previously [5,6,21]. Upon further increasing pressure above 4 GPa, the resistivity shows a remarkable drop at low temperature, which manifests a pressure-induced insulator-metal transition (MIT). It is noteworthy that the different pressure transmitting medium can give rise to different pressure environments for the sample. This pressure medium effect on sample is particularly serious in SmB_6, as reported by Derr et al. in Ref [35]. The MIT of the SmB_6 in a hydrostatic pressure environment (using an argon gas as pressure medium) is pushed up to 10 GPa, while in a quasi-hydrostatic pressure environment (using steatite [35–37] or NaCl in this study as pressure medium) the MIT occurs at ~4 GPa.

Interestingly, the onset temperature (T^*) of the resistance plateau exhibits a downward trend with increasing pressure, and disappears at ~4 GPa (Fig. 1c). Above 4 GPa, while the resistivity vs. temperature becomes metallic-like at low temperatures ($T < \sim 20$ K), it still exhibits insulating-like behavior at higher temperatures ($T > \sim 20$ K). This is so for pressures below ~10 GPa; only at even higher pressures (>10 GPa) does the system changes to metallic-like behavior over the entire measured temperature range (Fig. S1, Supplementary Information). In the pressure range investigated, no crystal structural phase transition is observed (Fig. S2, Supplementary Information), in agreement with the results reported [32,33,38]. This indicates that the pressure-induced resistance evolution stems from purely electronic physics.

To determine the nature of the ground state at 4 GPa and above, we fitted the resistivity-temperature (R-T) data from 0.3 to 4 K with the power law, $\rho(T) = \rho_0 + AT^n$ (where ρ_0 is the residual resistivity, A the electron-electron scattering coefficient and n the exponent), we find that below 0.7 K the R-T curve at 4 GPa clearly follows a Fermi liquid (FL) behavior with $n = 2$ (Fig. 2a). A linear R-T behavior at 4 GPa presents only in the temperature range of 1.5–4 K (Fig. 2a), in agreement with previous measurements at higher temperatures (>1.5 K) [21]. Within the temperature range of 0.7–1.5 K, n lies between 1 and 2. Our results reveal that the real ground state of SmB_6 at 4 GPa is a FL state, instead of a non-FL state. Our investigation of high-pressure resistance measurements at 4.5 GPa down to 0.03 K further confirms the FL ground state (Fig. S3, Supplementary Information). Fits to the R-T data measured down to 0.3 K for the pressures ranging from 5 to 19.6 GPa demonstrates that the T_{FL}, the temperature into the Fermi liquid regime, appears to increase linearly with pressure (Fig. 2b, c, Figs. S3, S4, Supplementary Information). Interestingly, the A coefficient in $\rho(T) = \rho_0 + AT^2$ as a function of pressure (as shown in Fig. 2d) shows that the A coefficient (3.3 μΩ cm/K^2) at 4 GPa is about 720 times larger than its value (0.0046 μΩ cm/K^2) at 19.6 GPa. Following the Kadowaki-Woods relation [39], this corresponds to an increase of the effective carrier mass (m^*) by a factor of ~27 as the pressure is reduced towards the transition pressure 4 GPa. We also fit the R-T data measured down to 0.03 K, and found that the value of the A coefficient is on the data line, suggesting that the A coefficient extracted from the R-T data measured down to 0.3 K should be very close to the one obtained from the R-T curve measured down to 0.03 K. By analogy with the behavior of heavy fermion metals [4,28], the striking divergence tendency in the effective mass with pressure on approach of 4 GPa signifies the destruction of Kondo entanglement (Kondo singlet) at the insulator-metal quantum phase transition.

4. Discussions and summary

The pressure-temperature phase diagram established from our transport data is shown in Fig. 3a. Three low temperature regions appear in this phase diagram. The region below 4 GPa represents the putative topological Kondo insulating (P-TKI) state characterized by the resistance plateau. In the intermediate-pressure region between 4 and 10 GPa, with decreasing temperature the sample shows a non-metallic behavior down to the T_P (the temperature of the resistance peak indicated by the arrow in Fig. S1, where the resistivity of the sample undergoes a change from non-metallic behavior to a metallic behavior) and then enters into a FL ground state below the T_{FL}. In the region above 10 GPa, the sample displays metallic behavior over the entire measured temperature range, and also shows a FL behavior at low temperature, where a long-range magnetic order is observed [30,31]. To further address the nature of the quantum phase transition at ~4 GPa, we performed Hall measurements at a fixed temperature of 1.7 K at different pressures up to ~20 GPa (Fig. 3b and Figs. S5–S7). The inverse Hall coefficient undergoes a large change across ~4 GPa. Comparing this low-temperature isothermal behavior with its counterparts at higher temperatures, we find that the crossover feature of the inverse Hall coefficient sharpens as the temperature is lowered (Fig. 3b, inset). Even though the Hall data is expected to contain contributions from both surface and bulk carriers, our results are compatible with a rapid change of the carrier number
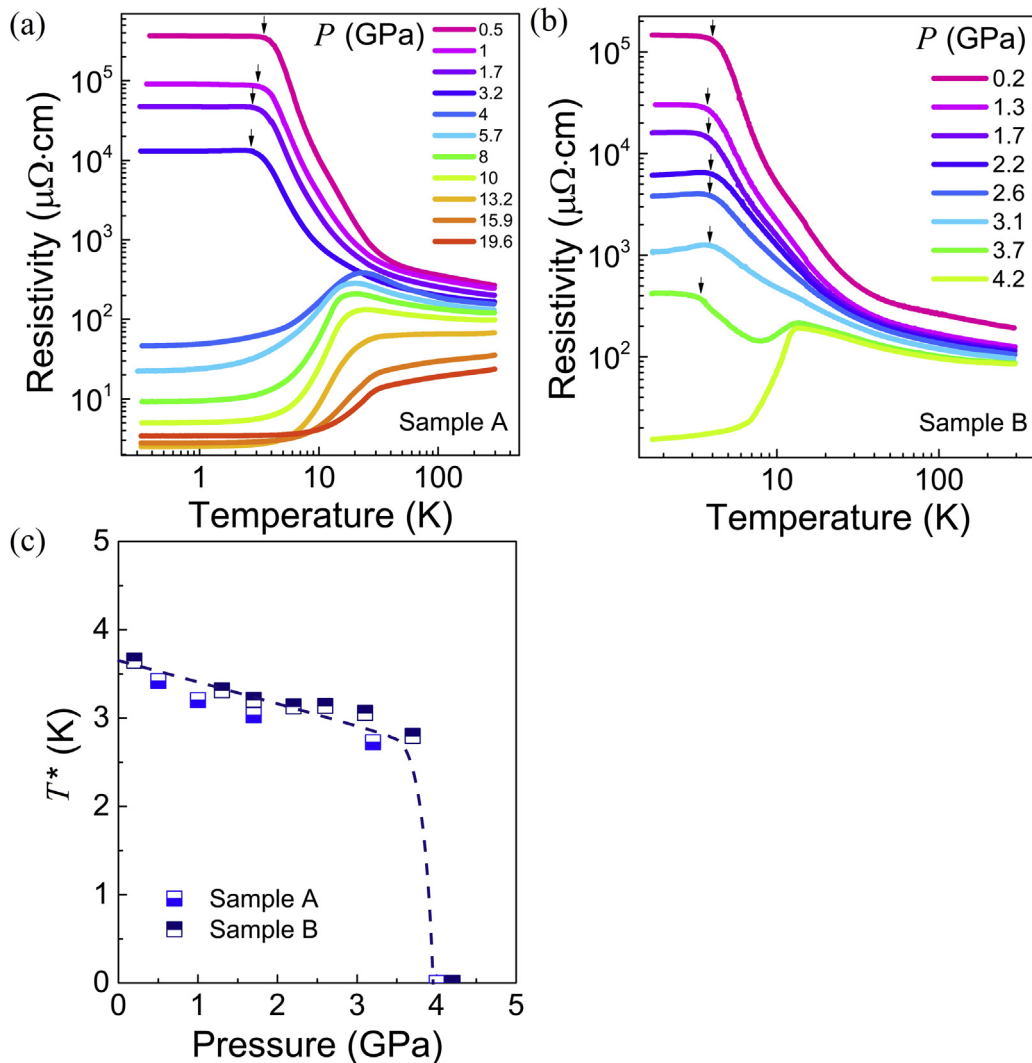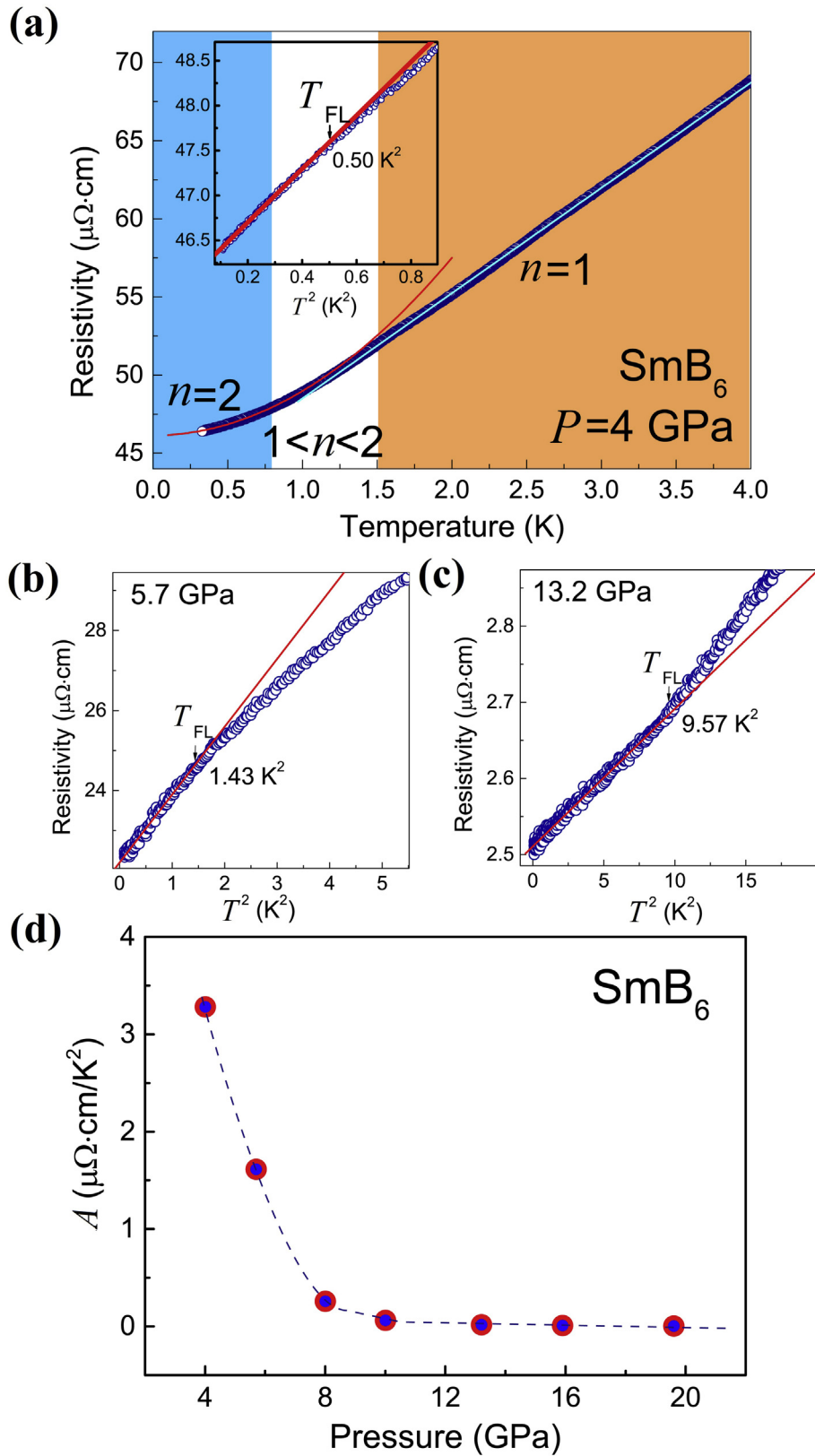
Fig. 1. (Color online) Resistivity-temperature data and onset temperature of resistance plateau (T^*) obtained at different pressures. (a) Temperature dependence of electrical resistivity in the sample A for pressures ranging from 0.5 to 19.6 GPa. (b) Resistivity as a function of temperature in the sample B for pressures ranging from 0.2 to 4.2 GPa. The arrow in (a) and (b) specifies T^*, the onset temperature for the resistance plateau. (c) Plot of T^* versus pressure extracted from the resistance measurements.

in the bulk at $\sim$4 GPa, which indicates the destruction of the Kondo state [4,27].

We made fits to our resistivity data by the Arrhenius equation (Fig. S8, Supplementary Information), and extracted the energy gap at each pressure value. In line with the multiplicity of the gaps, we identify two energy gaps E_l (low temperature gap) and E_h (high temperature gap), respectively. As shown in the inset of Fig. 3a, their ambient-pressure values are very consistent with the reported results determined by previous resistance measurements [6,21,22]. It is seen that both E_l and E_h decrease monotonically upon increasing pressure. As pressure is increased towards 4 GPa, the E_l decreases to zero. Simultaneously, the onset temperature (T^*) of the resistivity plateau that features the existence of the metallic surface state decreases with increasing pressure and vanishes at the critical pressure $\sim$4 GPa (Fig. 1a and b). Thus our high-pressure results reveal the intimate connection between T^* and E_l, which supports that the ground state (the resistivity plateau) at $T < T^*$ is protected by the energy gap E_l. Our results also suggest that the E_l gap *reflects* the hybridization gap developed upon the formation of a static Kondo-singlet in the ground state. While, the E_h gap remains finite across 4 GPa and gradually decreases upon further increasing the pressure towards $\sim$10 GPa. We therefore interpret

the E_h as a signifying for the onset of the dynamical Kondo hybridization, which exists at higher temperature.

For SmB$_6$, the unusual phenomena occur in a mixed valence state with f electron configuration between $4f^6$ and $4f^5 + 5d^1$. To understand the pressure-induced resistance behavior, the corresponding evolution of the two energy gaps and the ground state of the phases in the intermediate-pressure and high-pressure regions, we performed *in situ* high pressure synchrotron X-ray absorption measurements. Representative L$_{III}$-edge spectra collected at different pressures are presented in Fig. S9 (Supplementary Information). The mean valance (v) as a function of pressure is plotted in Fig. 3b. It can be seen that v increases with pressure. Particularly across 4 GPa, the mean v shows an increase from 2.55 to 2.62. The pressure-induced valence change leads us to suggest that an appropriate mixed valence state is crucial for the low temperature behavior in SmB$_6$. In the high pressure region above 10 GPa, we found that the mean valence is closed to 3+, *i.e.* the concentration of magnetic Sm^{3+} ions is dominant, which should promote the development of long-ranged magnetic order [40,41]. It is noted that the high-pressure valence measurements on SmB$_6$ were also carried out by Butch et al. as reported in Ref. [38], the tendency of the pressure-induced valence changes of Sm ions

Fig. 2. (Color online) Electrical resistivity as a function of temperature measured down to 0.3 K. (a) The blue solid are the plot of resistivity versus temperature obtained at 4 GPa. The data can be fitted by $\rho = \rho_0 + AT^2$ in the range below 0.7 K (red line) and by $\rho = \rho_0 + BT$ in the temperature range of 1.5–4 K (light blue), respectively. The low temperature part is zoomed in for a clear view (inset), indicating a Fermi-liquid ground state. (b) and (c) Electrical resistivity versus T^2 at 5.7 and 13.2 GPa, respectively. The highest temperature of the quadratic behavior is defined as the onset temperature (T_{FL}) of the Fermi-liquid state. (d) Pressure dependence of the A coefficient, showing a divergence tendency as the pressure approaches ~4 GPa.
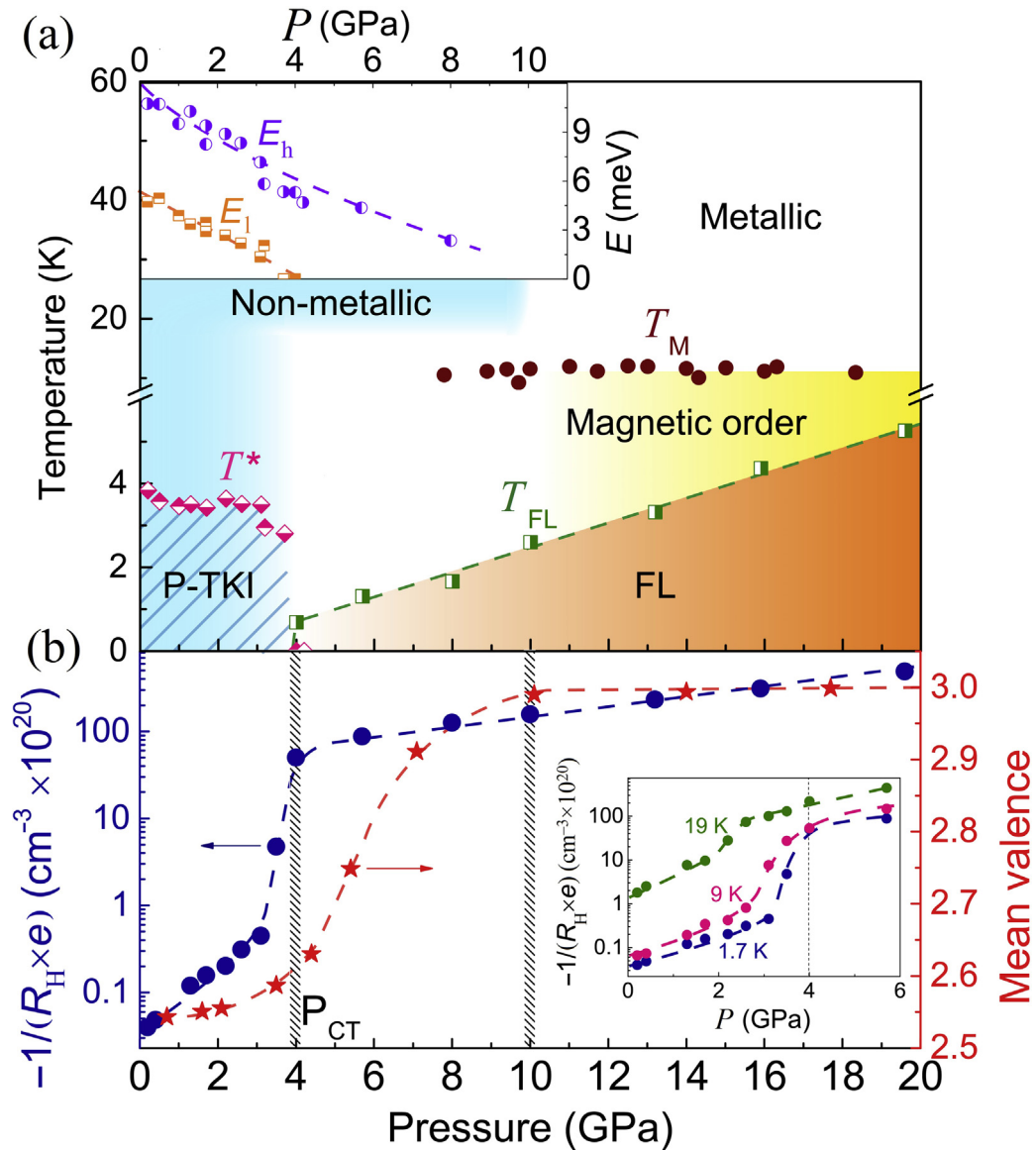
Fig. 3. (Color online) Summary of pressure dependence of temperature, inverse Hall coefficient and mean valence of SmB$_6$. (a) Phase diagram depicted by the pressure dependence of the onset temperature of the resistance plateau (T^*) and Fermi liquid (T_{FL}), respectively. Here P-TKI and FL represent the putative topological Kondo insulating state and Fermi liquid state, respectively. T_M stands for the magnetic transition temperature taken from Refs. [30,31]. The filled green square represents the T_{FL} determined from the resistance measurements down to 0.3 K and the filled green circle represents the T_{FL} determined from the resistance measurements down to 0.03 K. The inset displays pressure dependence of the two activation gaps E_l (low temperature gap) and E_h (high temperature gap), respectively. (b) Plots of inverse Hall coefficient (R_H) and mean valance of Sm ions versus pressure. The inset displays the inverse R_H as a function of pressure at different temperatures.

between our measurements and Butch's measurements is the same, *i.e.* both increase with pressure, though their value shows a deviation from ours. We attribute the deviation to the difference of the pressure transmitting mediums used in these two experiments. Our high-pressure X-ray absorption results are consistent with the previous nuclear forward scattering and specific heat measurements, in which a magnetic order phase is observed at pressure above 7 GPa [30,31]. The corresponding pressure dependence of the magnetic transition temperature (T_M), taken from Refs. [30,31], are also shown in the phase diagram (Fig. 3a). How this transition line evolves as the pressure is further decreased is an important issue that needs to be clarified by future experiments.

In summary, we have studied the exotic high pressure behavior of SmB$_6$ through comprehensive *in situ* high pressure measurements of resistance, Hall coefficient and synchrotron X-ray diffraction and absorption. From these measurements, we are able to

establish the pressure dependences of two energy gaps (the low temperature gap E_l and the high temperature gap E_h), the onset temperature of resistance plateau, the Fermi liquid temperature, the Hall coefficient and valence change of Sm ions, all up to 20 GPa. The real ground state of SmB$_6$ at 4 GPa is uncovered using our advanced high-pressure and low-temperature (0.3 K) cryostat, and an ultra-low-temperature (0.03 K) cryostat, to be Fermi-liquid state, instead of non-Fermi liquid state known before. We find a pressure-induced quantum phase transition from the ambient-pressure state of a possibly topological Kondo insulator to a Fermi-liquid state with a divergence tendency of the effective mass at ~4 GPa, which occurs in the background of mixed valence state, and we provide direct evidence for the destruction of the bulk Kondo hybridization state at this quantum phase transition. In addition, we find that the E_l gradually decreases with pressure and reaches zero at 4 GPa, which is accompanied by the

suppression of the resistance plateau, suggesting that the metallic surface state is protected by the existence of the E_1 gap. Our findings point towards an exciting prospect for studying topological electronic states in quantum critical materials settings.

Conflict of interest

The authors declare that they have no conflict of interest.

Acknowledgments

Appendix A. Supplementary data

Supplementary data associated with this article can be found, in the online version, at https://doi.org/10.1016/j.scib.2017.10.008.

References

[1] Young DP, Hall D, Torelli ME, et al. High-temperature weak ferromagnetism in a low-density free-electron gas. Nature 1999;397:412–4.
[2] Riseborough PS. Heavy fermion semiconductors. Adv Phys 2000;49:257–320.
[3] Coleman P. Heavy Fermions: Electrons at the Edge of Magnetism. Wiley; 2007. pp. 95–148.
[4] Si Q, Paschen S. Quantum phase transitions in heavy fermion metals and Kondo insulators. Phys Status Sol B 2013;250:425–38.
[5] Beille J, Maple MB, Wittig J, et al. Suppression of the energy gap in SmB6 under pressure. Phys Rev B 1983;28:7397–400.
[6] Cooley JC, Aronson MC, Fisk Z, et al. SmB6: Kondo insulator or exotic metal? Phys Rev Lett 1995;74:1629–32.
[7] Dzero M, Sun K, Galitski V, et al. Topological Kondo insulators. Phys Rev Lett 2010;104:106408.
[8] Lu F, Zhao J, Weng H, et al. Correlated topological insulators with mixed valence. Phys Rev Lett 2013;110:096401.
[9] Jiang J, Li S, Zhang T, et al. Observation of possible topological in-gap surface states in the Kondo insulator SmB6 by photoemission. Nat Commun 2013;4:3010.
[10] Kim DJ, Thomas S, Grant T, et al. Surface hall effect and nonlocal transport in SmB6: evidence for surface conduction. Sci Rep 2013;3:3150.
[11] Kim DJ, Xia J, Fisk Z. Topological surface state in the Kondo insulator samarium hexaboride. Nat Mater 2014;13:466–70.
[12] Rößler S, Jang TH, Kim DJ, et al. Hybridization gap and Fano resonance in SmB6. Proc Natl Acad Sci 2014;111:4798–802.
[13] Ruan W, Ye C, Guo M, et al. Emergence of a coherent in-gap state in the SmB6 Kondo insulator revealed by scanning tunneling spectroscopy. Phys Rev Lett 2014;112:136401.
[14] Luo Y, Chen H, Dai J, et al. Heavy surface state in a possible topological Kondo insulator: magnetothermoelectric transport on the (011) plane of SmB6. Phys Rev B 2015;91:075130.
[15] Syers P, Kim D, Fuhrer MS, et al. Tuning bulk and surface conduction in the proposed topological Kondo insulator SmB6. Phys Rev Lett 2015;114:096601.
[16] Wakeham N, Wang YQ, Fisk Z, et al. Surface state reconstruction in ion-damaged SmB6. Phys Rev B 2015;91:085107.
[17] Park WK, Sun L, Noddings A, et al. Topological surface states interacting with bulk excitations in the Kondo insulator SmB6 revealed via planar tunneling spectroscopy. Proc Natl Acad Sci 2016;113:6599–604.
[18] Hlawenka P, Siemensmeyer K, Weschke E, et al. Samarium hexaboride: a trivial surface conductor; 2015. arXiv: 150201542.
[19] Menth A, Buehler E, Geballe TH. Magnetic and semiconducting properties of SmB6. Phys Rev Lett 1969;22:295–7.
[20] Allen JW, Batlogg B, Wachter P. Large low-temperature Hall effect and resistivity in mixed-valent SmB6. Phys Rev B 1979;20:4807–13.
[21] Gabáni S, Bauer E, Berger S, et al. Pressure-induced Fermi-liquid behavior in the Kondo insulator SmB6: possible transition through a quantum critical point. Phys Rev B 2003;67:172406.
[22] Neupane M, Alidoust N, Xu SY, et al. Surface electronic structure of the topological Kondo-insulator candidate correlated electron system SmB6. Nat Commun 2013;4:2991.
[23] Zhang X, Butch N, Syers P, et al. Hybridization, inter-ion correlation, and surface states in the Kondo insulator SmB6. Phys Rev X 2013;3:011011.
[24] Li G, Xiang Z, Yu F, et al. Two-dimensional Fermi surfaces in Kondo insulator SmB6. Science 2014;346:1208–12.
[25] Tan BS, Hsu YT, Zeng B, et al. Unconventional Fermi surface in an insulating state. Science 2015;349:287–90.
[26] Yamamoto SJ, Si Q. Global phase diagram of the Kondo lattice: from heavy Fermion metals to Kondo insulators. J Low Temp Phys 2010;161:233–62.
[27] Pixley JH, Yu R, Paschen S, et al. Global phase diagram and momentum distribution of single-particle excitations in Kondo insulators; 2015. arXiv: 150902907.
[28] Park T, Ronning F, Yuan HQ, et al. Hidden magnetism and quantum criticality in the heavy fermion superconductor CeRhIn5. Nature 2006;440:65–8.
[29] Zhou Y, Kim DJ, Rosa PFS, et al. Pressure-induced quantum phase transitions in a YbB6 single crystal. Phys Rev B 2015;92:241118.
[30] Barla A, Derr J, Sanchez JP, et al. High-pressure ground state of SmB6: electronic conduction and long range magnetic order. Phys Rev Lett 2005;94:166401.
[31] Derr J, Knebel G, Lapertot G, et al. Valence and magnetic ordering in intermediate valence compounds: TmSe versus SmB6. J Phys Condens Matter 2006;18:2089.
[32] Nishiyama K, Mito T, Pristáš G, et al. Pressure-induced localization of 4f electrons in the intermediate valence compound SmB6. J Phys Soc Jpn 2013;82:123707.
[33] Paraskevas P, Martin B, Mohamed M. High-pressure structural anomalies and electronic transitions in the topological Kondo insulator SmB6. Europhys Lett 2015;110:66002.
[34] Mao HK, Xu J, Bell PM. Calibration of the ruby pressure gauge to 800 kbar under quasi-hydrostatic conditions. J Geophys Res 1986;91:4673–6.
[35] Derr J, Knebel G, Braithwaite D, et al. From unconventional insulating behavior towards conventional magnetism in the intermediate-valence compound SmB6. Phys Rev B 2008;77:193107.
[36] Demuer A, Holmes AT, Jaccard D. Strain enhancement of superconductivity in CePd2Si2 under pressure. J Phys Condens Matter 2002;14:L529.
[37] Klotz S, Chervin JC, Munsch P, et al. Hydrostatic limits of 11 pressure transmitting media. J Phys D Appl Phys 2009;42:075413.
[38] Butch NP, Paglione J, Chow P, et al. Pressure-resistant intermediate valence in the Kondo insulator SmB6. Phys Rev Lett 2016;116:156401.
[39] Kadowaki K, Woods SB. Universal relationship of the resistivity and specific heat in heavy-Fermion compounds. Sol State Commun 1986;58:507–9.
[40] Sun L, Wu Q. Pressure-induced exotic states in rare earth hexaborides. Rep Prog Phys 2016;79:084503.
[41] Wu Q, Sun L. Puzzle maker in SmB6: accompany-type valence fluctuation state. Rep Prog Phys 2017;80:112501.